In: *Proc. 29th Coastal Engineering Conference*, World Scientific Press, 2005*, pp. 2120-2132.*

NUMERICAL MORPHOLOGIC MODEL OF BARRIER ISLAND BREACHING

NICHOLAS C. KRAUS
U.S. Army Engineer Research and Development Center
Coastal and Hydraulics Laboratory
3909 Halls Ferry Road, Vicksburg, MS 39180, USA

KENTARO HAYASHI
Alpha Hydraulic Engineering Consultants Co., Ltd.
516-336, 9-14 Hassamu, Nishi-Ku
Sapporo, Hokkaido 063-0829, Japan

A numerical model of barrier island breaching is presented that is based on an assumed rectangular breach form. Sediment transport is calculated at the bottom and sides of the breach as driven by the Keulegan one-dimensional inlet hydrodynamics equations. Longshore transport is included and can close a breach. Multiple inlets to the same bay can be represented. The model is validated by comparison to laboratory data and to measurements of the 1980 breach at Moriches Inlet, Long Island, New York.

1. Introduction

Coastal barrier islands can breach during storms and times of elevated water level. Breaching is expected to become more prevalent with rise in sea level, erosion of the coast, and continued length of service of jetties that cause erosion along the adjacent beaches. Quantitative predictive tools are needed to assess vulnerability of coastal barriers, design breach prevention, develop beach-closure plans, estimate the fate of a breach, and evaluate the consequences of a breach to the neighboring beach, bay, and inlets sharing the same bay system. Coastal breaching processes and its engineering implications are reviewed by Kraus et al. (2001), Kraus and Wamsley (2002), and Kraus (2003).

A coastal breach is a new opening in a narrow landmass such as a barrier island or barrier spit that allows flow between the water bodies on each side. Initial breaching is characterized by strong cross-barrier (cross-shore) transport that creates the new opening. During initial breach growth, which is usually rapid because of disequilibrium in water level or flow rate, the cross-barrier sediment transport rate is expected to be much greater than the longshore transport rate. As the breach depth and width approach equilibrium, or the causative mechanism (storm surge, elevated bay water level, strong river flow)

subsides, the cross-barrier flow rate decreases, and longshore sediment transport can partially or completely fill the breach. Kraus (1998) presents a mathematical model for calculating inlet (or breach) cross-sectional area about equilibrium in response to changes in discharge through the opening and longshore sediment transport.

This paper describes a numerical model of incipient breaching of an alluvial coastal barrier. The numerical model extends the analytical morphologic models of Kraus (1998, 2003) by coupling a sediment transport equation driven by one-dimensional (1-D) inlet flow equations to calculate breach growth under an assumed rectangular geometry. The morphologic model is first reviewed and then extended to include forcing by tidal hydrodynamics, longshore sediment transport, and possibility of multiple breaches and inlets. The numerical model is tested by comparison to published physical model data and to data from the 1980 breach adjacent to Moriches Inlet, Long Island, New York.

2. Review of Analytical Breaching Model

The model proceeds from the continuity equation expressed for an assumed rectangular breach cross-sectional geometry. Because of the assumption of a specified geometry, the model is termed a "morphologic model." In the original model (Kraus 2003), the simple form of a rectangular barrier island was specified, as depicted in Fig. 1. The rectangular barrier island has cross-shore width L, and the breach has width x and depth z measured from the crest of the barrier. A net transport rate at the bottom Q_B in short period of time Δt erodes a bottom layer of uniform thickness Δz, and a transport rate Q_S on each side erodes each side as a layer of uniform thickness Δx.

For such a rectangular barrier island and rectangular breach, the continuity equation for sediment volume on one side and on the bottom yields, respectively,

$$\frac{dx}{dt} = \frac{Q_S}{Lz}, \quad x_0 > 0, \tag{1}$$

and

$$\frac{dz}{dt} = \frac{Q_B}{Lx}, \quad z_0 > 0, \tag{2}$$

in which x_0 and z_0 are the initial width and depth of the region in the barrier island where the breach forms. Eqs. (1) and (2) are two coupled first-order non-linear differential equations governing breach width and depth, respectively.

In the original morphologic model (Kraus 2003), the transport rates were parameterized as $Q_S = \hat{Q}_S(1 - x/x_e)$ and $Q_B = \hat{Q}_B(1 - z/z_e)$, in which $\hat{Q}_S$ and $\hat{Q}_B$ are constant maximum rates assumed to occur at the start of the breach, and x_e and z_e are values of the breach width and depth at equilibrium with the breach-forcing conditions. Closed-form solution of the two equations was found possible if $\hat{Q}_B$ and $\hat{Q}_S$ equaled a constant rate $\hat{Q}$, leading to solutions of the form $x = x_e\left[1 - f(x)\exp(-t/\tau)\right]$ and $z = z_e\left[1 - g(z)\exp(-t/\tau)\right]$. These solutions describe an exponential growth toward equilibrium at a rate governed by the morphologic time scale $\tau = x_e z_e L/\hat{Q}$. Eqs. (1) and (2) possess characteristics encountered in chaos theory. Therefore, the solution at early stages strongly depends on the initial condition, contained in the functions *f* and *g*, but reaches the same value in exponential growth toward equilibrium.

The original morphologic model represents the macro-scale process of breach growth. The solution indicates time-dependent breach dimensions are controlled by seven variables: initial width and depth of the breach, equilibrium width and depth of the breach, width of the barrier island, and maximum or initial net sediment transport rates at the bottom and sides of the breach.

The original model was limited in not accounting for the current that transports sediment through the breach. The breaching model is extended here by incorporating a 1-D inlet hydrodynamic model to calculate sediment transport, as well as including longshore sediment transport and wave set up.

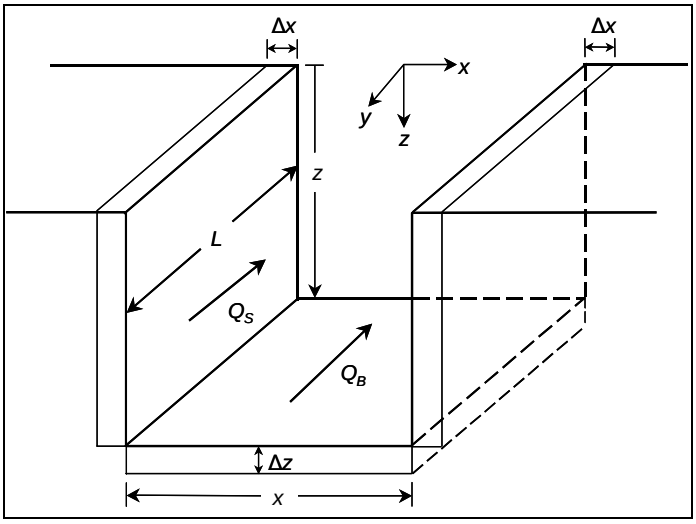

Figure 1. Definition sketch for rectangular barrier island.

2.1. *Morphologic Model with 1-D Hydrodynamic Forcing*

The classical depth-averaged 1-D inlet hydrodynamics equations of Keulegan (1967) are implemented. These are the momentum equation,

$$\frac{\partial U}{\partial t} + \frac{g}{L}\left(\eta_B - \eta_O\right) + \left(K_{en} + K_{ex} + \frac{2c_f L}{R_H} \right) \frac{|U|U}{2L} = 0 \,, \tag{3}$$

and the continuity equation,

$$A_C U = A_B \frac{d\eta_B}{dt} \,, \tag{4}$$

in which U = depth-averaged and inlet-length integrated current velocity, A_C = breach or inlet channel cross-sectional area below mean sea level (msl), t = time, g = acceleration of gravity, η_B and η_O = water surface deviations from msl in the bay and in the ocean, respectively, K_{en} and K_{ex} = entrance and exit losses, respectively, c_f = bottom friction coefficient taken here by Mannings formula $c_f = gn^2 / h^{1/3}$ in which n = Mannings coefficient typically set as 0.025 s/m$^{1/3}$, R_H = hydraulic radius of the inlet, and A_B = surface area of the bay. The assumptions of an idealized Keulegan inlet apply, such as vertical walls in the bay, and sufficiently small bay area to allow the bay surface to move up and down uniformly in response to tidal flow. In the breach model, the breach cross-sectional area expressed in Eq. (4) is time dependent. Eqs (3) and (4) are solved for U and η_B, respectively.

For the situation of multiple inlets and breaches, if the openings do not directly interact (with the other Keulegan assumptions still holding), U in Eq. (3) can be replaced by U_i and A_C by $(A_C)_i$ for the i^{th} opening among N total. Eq. (4) generalizes to:

$$\sum_{i=1}^{N} (A_c)_i U_i = A_B \frac{d\eta_B}{dt} \,. \tag{5}$$

If waves are present, in addition to increasing the bottom shear stress, breaking waves produce set up, calculated in the model by standard equations.

2.2. *Sediment Transport*

The sediment transport rate at the bottom is calculated by total load formula given by Watanabe et al. (1991),

$$q_B = \alpha \frac{(\tau_m - \tau_c)}{\rho g} U \quad , \tag{6}$$

in which α = empirical coefficient of order unity, $\tau_m = c_f \rho \langle |U| U \rangle$ is the time-averaged bottom shear stress, τ_c is the critical shear for sediment motion, and ρ is the density of water. In the presence of waves, the quadratic dependence of the shear stress τ_m is expressed by the Nishimura (1988) approximation.

Field observation indicates that the rapidly flowing water through a breach will remove material both by direct shear on the sides of the opening and by notching of the side, causing collapse of the material above the notch. This complex process is simply represented as a fraction of the total transport at the bottom as,

$$q_S = \beta q_B \quad , \tag{7}$$

where the value β = 0.7 is typically assigned.

2.3. *Numerical Solution Method*

Eqs. (3) and (4) are solved by a trapezoidal finite-difference method, and for field conditions a time step of 10 sec gave good results. Longer time steps, for example, 60 sec, are possible. However, in some situations, physically generated transients can be generated following rapid changes in water level and opening of a breach. A 10-sec time step was found to control these transients. After the velocity is obtained at time step *n*, transport rates are calculated and substituted into explicit finite-difference forms of Eqs. (1) and (2). The solution then proceeds forward.

2.4. *Layered Barrier Island*

The original model (Kraus 2003) developed solutions for a rectangular barrier island (Fig. 1). Although a rectangle is a reasonable first approximation, barrier islands, especially those prone to breaching, have a pyramidal or curved cross section. In a numerical solution, such a shape can be represented by a series of stacked rectangles to give a layered barrier island shape (Fig. 2). As the breach deepens, new layers are opened in the model, giving a new length *L* and surface area on the sides for calculating sediment transport. A similar extension of the model allows representation of island width to represent a common feature of narrowing of a barrier island where it may be more vulnerable to breaching.

3. Results

This section compares model calculations with physical model data of dike breaching to demonstrate general properties of the model, and with field data for a dual opening situation of a breach that formed next to an inlet jetty.

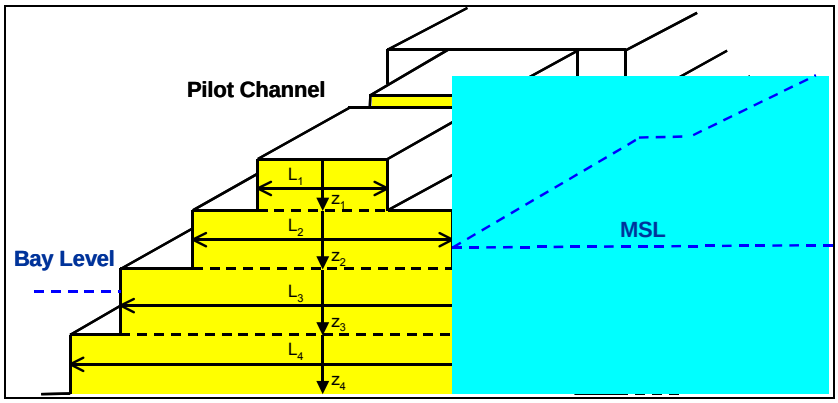

Figure 2. Layered barrier island cross section and horizontal section.

3.1. *Comparisons to Physical Model*

De Looff et al. (1996) report results of a physical model of a sand dike installed in a basin to investigate growth in breach width for various dike configurations. The breach was initiated by opening a small pilot channel at the top of the dike. Breach width, upstream water level, and surface water velocity by were recorded for eight cases with different cross-sections. In the present study, three cases (T2, T4, and T7) were examined to investigate the dependence of the numerical model on initial sand volume. Fig. 3 shows the initial cross-sections for T2, T4, and T7. Several layers were defined to represent the dike. With T4 as the standard dike, Case T2 had smaller sand volume, whereas T7 had larger volume.

Calibration of the present breaching model was performed by adjusting the sediment transport parameters for Case T4, which yielded $\alpha = 2.5$ and $\beta = 0.5$ for a best fit to the measurements. With these parameters fixed, simulations were run for Cases T2 and T7. The calculations, Fig. 4, follow the trend of the observations, with the width growing faster for dikes with less volume. Measurements of depth were not available to quantitatively judge performance of the numerical model; lack of information on measured depth and downstream water level make quantitative comparison infeasible.

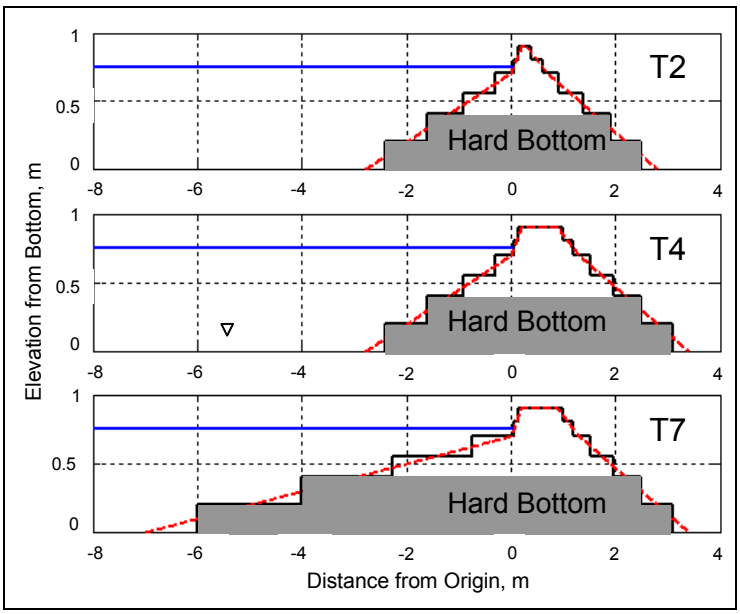

Figure 3. Cross sections T2, T4, and T7.

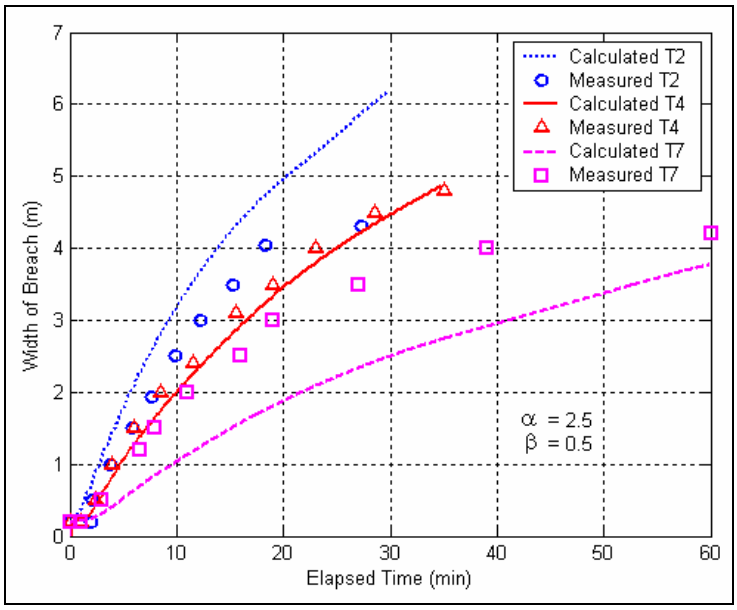

Figure 4. Calculations and measured breach width.

De Looff et al. (1996) identified a critical water velocity of 1.0 m/sec at which growth in breach width halted, similar to that found for stable inlets in the field (Bruun 1966). The numerical model reproduced this behavior (Fig. 5), with the calculated velocity rising rapidly as the breach first opened, then gradually decreasing to approach 1.0 m/sec as the breach widened and deepened.

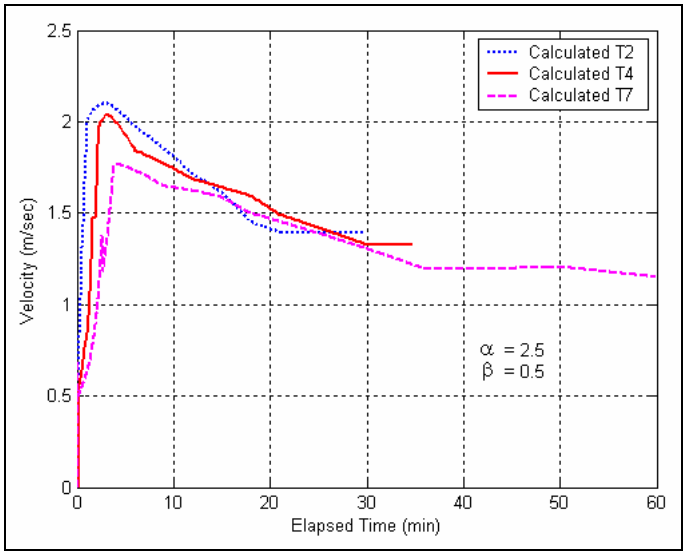

Figure 5. Calculated velocity in breach experiment of DeLoof et al. (1996).

3.2. *Moriches Inlet Breach, 1980*

With reasonable results obtained from comparison of model predictions and laboratory data, a study was performed to simulate field observations. The model was enhanced to include wave setup, longshore sediment transport calculated with the CERC equation, and breach channel infilling by deposition. Kraus and Hayashi (in preparation) describe these enhancements.

On 14-16 January 1980, a storm opened a breach at the narrowest point in the barrier island about 310 m east of the east jetty in Moriches Inlet, NY (Schmeltz et al. 1982; Sorenson and Schmeltz 1982). Wave data taken from the nearby Wave Information Study hindcast Station 111 are plotted in Fig. 6. The storm of mid January 1980 that opened the breach was followed by several winter storms, including a large storm in mid March. Kraus (2003) summarizes previously reported information about this breach. To obtain additional data on breach response, seven aerial photographs taken after the breach opened were analyzed in a GIS to obtain the breach width (Fig. 7).

The initial pilot channel was assigned 50-m width and 0.25-m depth (from the top of barrier island) based upon information obtained from local experts who monitored the breach. Inspection of aerial photographs indicated the breach reached the east jetty in early May 1980, and maximum breach width of 850 m was achieved sometime between 18 July and 25 August 1980. After maximum width was achieved, the breach narrowed slightly, attributed to longshore sediment transport directed toward the west, which initiated spit growth to the west. Depth across the breach was irregular, and shallow areas to the east were not surveyed. Therefore, as representative depths, the area-averaged value and the minimum value were compiled for comparison to calculations.

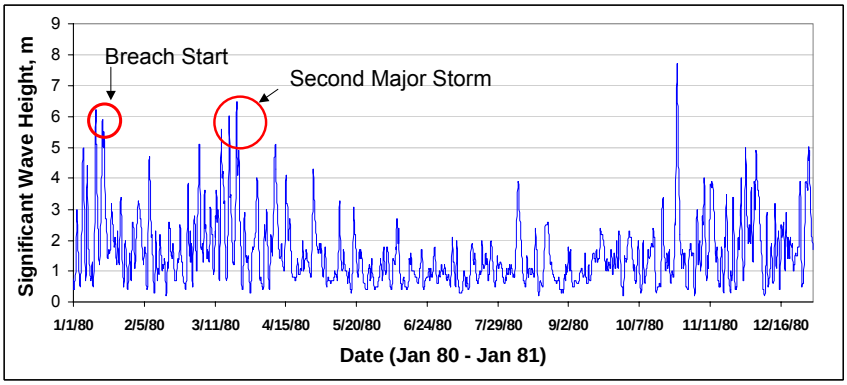

Figure 6. WIS wave record, Station 111, 1980

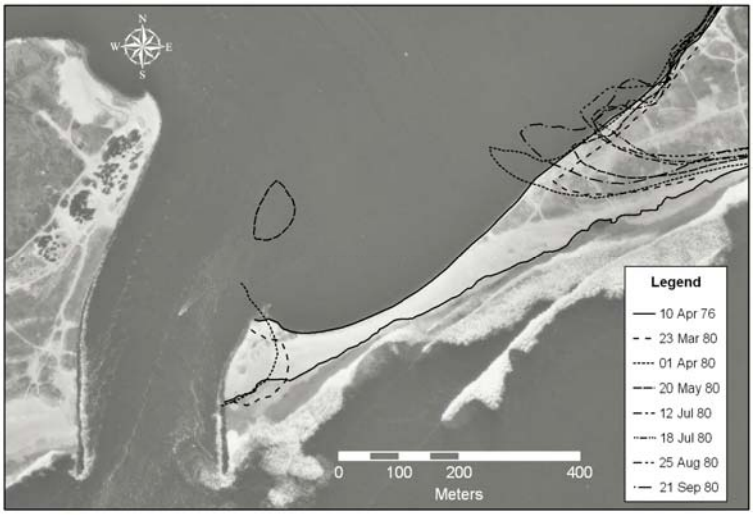

Figure 7. Moriches Inlet breach development (photograph April 1976).

The barrier island was divided into three horizontal sections. The narrowest initial barrier island cross-section was specified according to an interview with Mr. Gilbert Nersesian, former senior coastal engineer at the U.S. Army Engineer District, New York. Width elsewhere was estimated according to an April 1976 aerial photograph (most recent photograph available before the breach). Water level was specified from the National Ocean Service Battery gauge at the southern tip of Manhattan, NY. The longshore sediment transport rate calculated from the CERC formula was driven by WIS data, calibrated by requiring an annual net rate of 250,000 m^3/year to the west. Model calibration parameters that produced the best results were $\alpha = 0.05$ and $\beta = 50$.

The model was run for 280-day simulation time starting 13 January 1980. Several days later, a breach was calculated to occur on the lowest barrier section. Fig. 8 plots a filtered envelope of the calculated current velocity in the inlet and breach. The velocity exceeded 2.5 m/sec when the simulated breach opened. After the storm subsided, tidal exchange between ocean and bay continued to enlarge the breach section. Over time, velocities in both the inlet and breach became smaller, with the breach section becoming another inlet. Flow in the breach was calculated to be flood biased, whereas flow in the inlet was ebb biased, produced by the non-linear friction term in Eq. 1. The calculated current is compatible with that reported by Schmeltz et al. (1980), who document a velocity of 1.5 - 2.1 m/sec in the breach section.

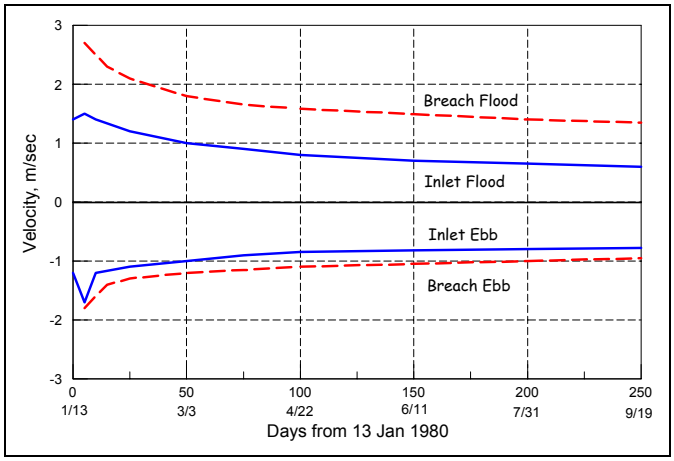

Figure 8. Filtered envelopes of current velocity in breach and inlet.

Calculated breach width and depth are plotted in Fig. 9 and Fig. 10, together with the measurements. The simulated breach reached the east jetty in

May, and the model automatically shut down half the breach side erosion at that time. Rapid initial growth of the breach is well reproduced, and calculated breach width and depth approach equilibrium. Prior to the March 1980 severe storm, the simulated breach appeared to begin approaching an equilibrium state. Subsequent storms (Fig. 6) continued deepening and opening the breach.

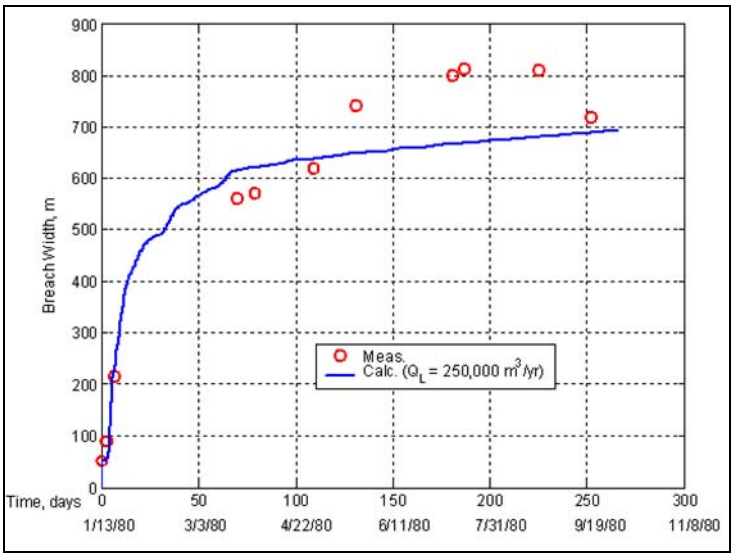

Figure 9. Calculated breach width compared to measurements.

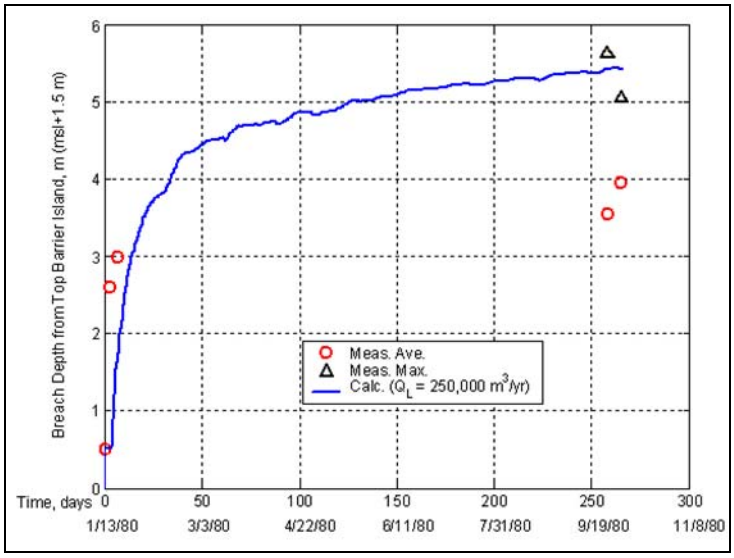

Figure 10. Calculated breach depth compared to measurements.

The model underestimates breach width at Moriches Inlet. This is attributed to the aerial photographs giving a maximum width that includes a broad shallow area on the east side of the breach that could not be reached by survey boat. The simulation better reproduces maximum breach depth than the average value, which again contains contributions that had to be estimated for a large reach of shallow water not surveyed.

Simulations were also performed for larger and smaller longshore sediment transport rates Q_L than the 250,000 m^3/year specified as a representative value. These sensitivity tests indicated that the breach would not have closed even under unusually large potential infilling by longshore transport.

4. CONCLUDING DISCUSSION

A morphologic model of coastal barrier breaching was developed and shown to reproduce trends in breach width documented in a dike-burst laboratory experiment and in measured width and depth of the 1980 breach, Moriches Inlet, NY. For the Moriches Inlet breach, hydrodynamics in both the existing inlet and the breach opening were simulated simultaneously with evolution of the breach.

The model balances erosion produced by tidal (and other) flow through a breach with input by longshore transport, which would tend to close the breach. In the present version of the model, closure occurs only by depth infilling and not by spit encroachment. The breach model runs rapidly, and numerous tests indicated the model to be robust in numerical stability and in producing reasonable results.

Breach opening depends directly on accuracy of data on the initial condition of the barrier island, in particular, about the lowest and narrowest section, and on the water level (tide and surge) and wave conditions. It was found that wave setup during storms can significantly increase water level at the site of a potential breach and exert strong control over breach opening and development.

Acknowledgments

This paper was prepared as an activity of the Coastal Inlets Research Program, Inlet Channels and Morphology Work Unit, U.S. Army Corps of Engineers (USACE). We would like to express appreciation to Dr. Henk Steetzel of Alkyon Hydraulic Consultancy & Research and to Dr. Paul Visser of the Delft University of Technology for providing supplementary information on the physical model dike experiments. Mr. Gil Nersesian, formerly of the

USACE New York District, and Mr Edward Schmeltz, Senior Vice President at DMJM + Harris, are thanked for providing supplemental information on the 1980 Moriches Inlet breach and for answering many questions. We appreciate a critical review of this paper given by Mr. Ty Wamsley, of the U.S. Army Engineer Research and Development Center, Coastal and Hydraulics Laboratory. Permission was granted by Headquarters, USACE, to publish this information.

References

Bruun, P. 1966. *Tidal Inlets and Littoral Drift.* University Book Co., Oslo, Norway, 193 pp.

De Looff, H., Steetzel, H. J., and Kraak, A. W. 1996. Breach Growth: Experiments and Modelling. *Proc. 25th Coastal Eng. Conf.*, ASCE, 2,746-2,755.

Keulegan, G. H. 1967. Tidal Flow in Entrances: Water Level Fluctuations of Basins in Communication with the Seas. Committee on Tidal Hydraulics Technical Bulletin No.14, U.S. Army Engineers Waterways Experiment Station, Vicksburg, MS.

Kraus, N. C. 2003. Analytical Model of Incipient Breaching of Coastal Barriers. *Coastal Eng. J.*, 45(4), 511-531.

Kraus, N.C., and Hayashi, K. (in preparation). Regional Model of Barrier Island Breaching.

Kraus, N. C., Militello, A., and Todoroff, G. 2002. Barrier Breaching Processes and Barrier Spit Breach, Stone Lagoon, California, *Shore & Beach* 70(4), 21-28.

Kraus, N. C., and Wamsley, T.V. 2003. Coastal Barrier Breaching, Part 1: Overview of Breaching Processes, ERDC/CHL CHETN IV-56, U.S. Army Engineer Research and Development Center, Vicksburg, MS. http://chl.wes.army.mil/library/publications/chetn.

Nishimura, H. 1988. Computation of Nearshore Current. In: *Nearshore Dynamics and Coastal Processes*, K. Horikawa, ed., University of Tokyo Press, Tokyo, Japan, 271-291.

Schmeltz, E. J., Sorensen, R.M., McCarthy, M. J., and Nersesian, G. 1982. Beach/Inlet Interaction at Moriches Inlet, *Proc. 18th Coastal Eng. Conf.*, ASCE, 1,062-1,077.

Sorensen, R. M., and Schmeltz, E. J. 1982. Closure of the Breach at Moriches Inlet, *Shore & Beach* 50(4), 22-40.

Watanabe, A., Shimuzu, T., and Kondo, K. 1991. Field Application of a Numerical Model of Beach Topography Response. *Proc. Coastal Sediments '91*, ASCE Press, 1814-1928.